Intersublevel optical transitions in InAs nanocrystals probed by photoinduced absorption spectroscopy: The role of thermal activation

D. Krapf,[1] S.-H. Kan,[2] U. Banin,[2] O. Millo,[3] and A. Sa'ar[1,3,*]

[1]*Department of Applied Physics, The Hebrew University of Jerusalem, Jerusalem 91904, Israel*
[2]*Department of Physical Chemistry, The Hebrew University of Jerusalem, Jerusalem 91904, Israel*
[3]*Racah Institute of Physics, The Hebrew University of Jerusalem, Jerusalem 91904, Israel*

Optical transitions between the quantized sublevels of colloidally synthesized InAs nanocrystals have been revealed using infrared photoinduced absorption spectroscopy. Two different groups of intersublevel transitions were observed. Using a correlation between the measured transition energies and experimental data obtained by scanning tunneling microscopy and photoluminescence excitation spectra, we have identified one group to be related to interconduction transitions while the other is related to intervalence transitions. However, in contrast to conduction intersublevel transitions that appear at all temperatures, we have found that the valence intersublevel transitions are thermally activated and cannot be observed at temperatures below 100 K. This behavior can be explained by assuming a three-level system model for the valence band. We propose two possible explanations for our findings; the first is based on the assumption of well-defined envelope-state symmetry relations while the second attributes the thermal activation process to the presence of shallow surface localized hole states.

Many of the electronic properties of colloidally synthesized semiconductor nanocrystals make them an ideal system for the study of quantum confinement effects in the strong confinement regime.[1–4] With the decreasing size of these nanocrystals their optical and electronic properties are expected to modify from those of bulk semiconductors into atomiclike properties of artificial molecules. One of the most significant features of carriers (electrons and holes) confinement in all three dimensions is the quantization of the energy bands (conduction and valence) of the bulk semiconductor into a discrete set of energy sublevels similar to those of isolated atoms and molecules. Several techniques have been utilized recently to probe size quantization in semiconductor quantum dots (QDs). For example, optical techniques such as photoluminescence[5] (PL), PL excitation[6,7] (PLE), and magneto-optics[8] were used to probe ultranarrow optical interband transitions.[9] Magnetotunneling[10] and scanning tunneling microscopy[11] (STM) have also been utilized to probe and spatially image the lowest wave functions of QDs.

Another powerful technique that can directly probe energy sublevel quantization in both the conduction and the valence bands of QDs is infrared (IR) intersublevel (ISL) absorption spectroscopy.[12–14] ISL absorption spectroscopy is related to optical transitions between sublevels lying in the same band (either conduction or valence). These transitions, which do not exist in bulk semiconductors, are a direct manifestation of quantization effects in QDs. Furthermore, since ISL absorption is essentially related to transitions between the envelope states of the sublevels, they are very sensitive to the spatial symmetry of the states. Over recent years there has been a great deal of discussion concerning the spatial symmetry of colloidally synthesized semiconductor QDs.[7,15–17] These QDs are characterized by a nearly perfect spherical shape that should be reflected in their electronic properties. However, it has been argued that the asymmetry associated with the underlying local Bloch states of binary semiconductors such as InAs and InP should play a crucial role in small spherical QDs.[15] Furthermore, this asymmetry yields a different type of energy sublevel hierarchy, particularly in the valence band, as calculated by either the $\vec{k}\cdot\vec{p}$ (Refs. 17 and 18) or the pseudopotential method.[15]

In this report, we describe remarkable phenomena associated with ISL transitions in colloidally synthesized InAs QDs. We have observed two different, well-resolved, absorption lines that are assigned to conduction and valence ISL transitions. The measured ISL energies follow size dependent scaling laws as expected from electronic structure calculations. Furthermore, the measured ISL transition energies show excellent agreement with both STM and PLE spectroscopic data, thus confirming our interpretation.[11] However, we have found opposite temperature evolution of the conduction and valence ISL transition strengths, indicating that the valence ISL (VISL) transition is thermally activated as opposed to the conduction-ISL (CISL) transition. This behavior can be attributed to either well-defined envelope-state symmetry relations (and selection rules) or to a contribution of optically active surface state below the QD energy band gap.

InAs nanocrystals were prepared by a colloidal chemical synthesis described elsewhere.[19] Narrow size distributions of nanocrystals with average radii from 1.4 nm up to 3.2 nm were dispersed from a solution on a GaAs substrate for further manipulation. Low temperature measurements were performed using a continuous flow, liquid helium cryostat allowing temperature control over the 4–300 K range. Notice that linear ISL absorption measurements cannot be applied to colloidal nanocrystals since a technology to intentionally dope these QDs has not been developed yet. Therefore, we have used IR photoinduced absorption (PIA) spectroscopy where a pump Ar^+ laser operating at 488 nm, generates electron-hole pairs (excitons) in the nanocrystals and a weak,
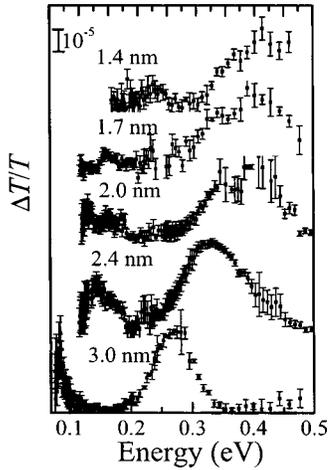
FIG. 1. Room temperature PIA spectra of InAs nanocrystals with radii from 1.4 nm to 3.0 nm.

IR blackbody source, has been used to probe ISL transitions of photoexcited carriers. The IR probe beam was dispersed by a 1/8 m IR spectrometer and detected by either HgCdTe or InSb liquid nitrogen cooled IR detectors covering the 2.5–16 μm spectral range. Differential transmission (ΔT) was measured by mechanical modulation of the pump beam using a lock-in detection technique and was normalized to the linear transmission (T) to yield the PIA signal as $\Delta T/T$. This technique has previously been utilized to resolve inter-subband transitions in semiconductor quantum wells[20] and quantum wires.[21]

Room temperature PIA spectra taken for InAs QDs of different radii are shown in Fig. 1. For all nanocrystal sizes we have observed two PIA absorption lines that are blue-shifted with decreasing radius of the nanocrystals, as expected from the quantum confinement picture. Furthermore, a comparison of the measured PIA peak energies with those obtained by STM and PLE spectroscopy (described in Ref.

11) is shown in Fig. 2. It can be seen that the measured PIA peak energies form two groups of ISL transition energies; the higher in energy is assigned to CISL transitions while the lower in energy is assigned to VISL transitions. The excellent correlation between the measured ISL energies by either technique can clearly be seen. Furthermore, our interpretation of the higher (lower) ISL transitions as CISL (VISL) transitions, as expected from the effective mass theory, is confirmed by the STM measurements, which are sensitive to carrier polarity.
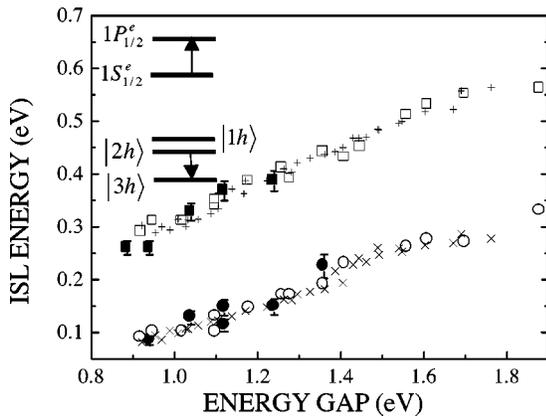

FIG. 2. ISL transition energies measured by PIA (full squares and circles), STM (open squares and circles), and PLE (crosses) versus the QD energy band gap. The distinction between two groups of CISL (upper data line) and VISL (lower data line) and the excellent correlation between the data obtained by all techniques can clearly be seen. The inset shows schematically the sublevel structure with the arrows representing the ISL optical transitions.
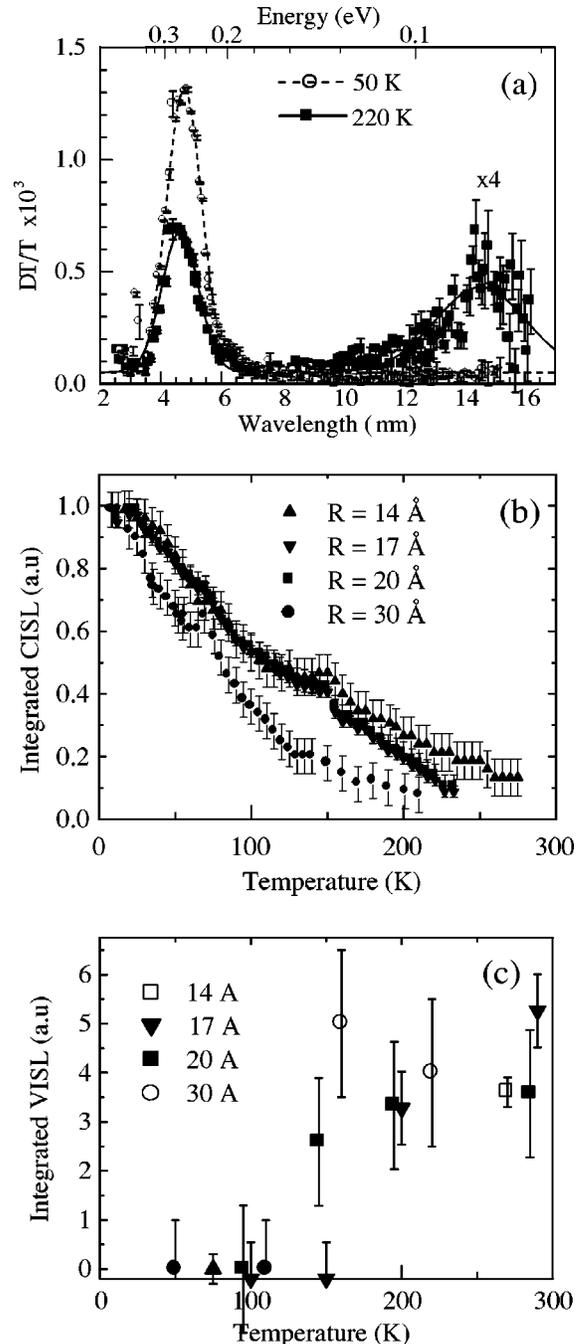
FIG. 3. (a) PIA spectra measured at 50 K (empty circles) and 220 K (full squares) for 3.0 nm radius InAs QDs. (b–c) Integrated PIA for CISL (b) and VISL (c) transitions vs temperature.
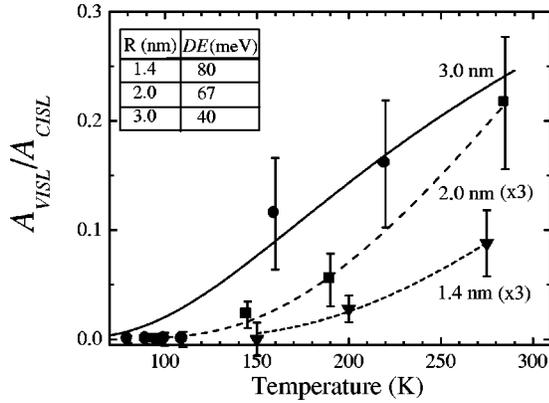
FIG. 4. The ratio between VISL and CISL integrated PIA versus temperature for three different sizes of InAs QDs. The lines represent the best fit of the experimental data to Eq. (1), while the table in the inset summarizes the activation energies deduced from this fitting procedure.

Next, the temperature dependence of the various PIA spectra was studied. In Fig. 3(a) we show typical PIA spectra at 50 K and 220 K of the 3 nm in radius InAs QD sample. While at 220 K (and room temperature, see Fig. 1) we observed two PIA lines at 260 meV (4.8 μm) with a full width at half maximum (FWHM) of 60 meV and a second PIA line at 85 meV (14.6 μm) with FWHM of about 13 meV, at low temperatures the low energy PIA line disappears. A similar phenomenon has been observed for all sizes of InAs QDs. Following our ISL transition identification (see Fig. 2) we conclude that the CISL transitions persist at all temperatures while the VISL transitions are thermally activated. To follow this activation process we plot in Figs. 3(b) and 3(c) the integrated PIA (i.e., the area below each PIA line) for both ISL transitions versus temperature. It can be seen that, while the CISL transitions monotonically increase with decreasing temperature, the VISL transitions diminish at temperatures below ~ 100 K.

Let us now discuss the origin of the ISL transitions observed in our experiments and the sublevels involved in these transitions. To this end, we will follow the $\vec{k} \cdot \vec{p}$ notation[17] for QDs (which assumes a perfect spherical symmetry) where the sublevel's wave functions are designated by nL_F, with n being the principal quantum number of the state, $\vec{F} = \vec{J} + \vec{L}$ is the total angular momentum that is composed of the envelope angular momentum L and the Bloch angular momentum J (which is also composed from a local orbital angular momentum and a spin). Notice also that spin-orbit interaction could couple states with $\Delta L = \pm 2$; however, for our purpose L denotes the lower envelope angular momentum.[22] The strongest electric dipole allowed ISL transitions occur between sublevels of the same Bloch orbital. Therefore, assuming small mixing between Bloch orbitals, we take $\Delta J = 0$ and $\Delta L = \pm 1$ (due to the well-defined symmetry of the envelope states) for ISL transitions. The lowest allowed CISL transition that is observed in our experiments is assigned to the $1S_{1/2}^e \rightarrow 1P_{3/2}^e$ ISL transition, with $1S_{1/2}^e$ being the ground sublevel for conduction electrons; see the inset to Fig. 2. This finding is supported by STM wave function imaging[11] as

well as theoretical calculations.[7,15] Applying similar arguments to the VISL transitions is more complicated, mainly due to heavy-hole light-hole mixing. However, our findings suggest that the valence sublevels structure can be described by a three-level system model with $|1h\rangle$, $|2h\rangle$, and $|3h\rangle$ denoting the ground and first and second excited hole states respectively. Assuming now that the observed VISL transition in our experiment is related to the $|2h\rangle \rightarrow |3h\rangle$ transition provides a nice and simple explanation to our findings of a VISL transition that is activated by the thermal population of the first excited state. Furthermore, denoting by N_1 and N_2 the populations of the $|1h\rangle$ and the $|2h\rangle$ sublevels, respectively we have $N_2/N_1 \cong g \exp(-\Delta E/kT)$, where ΔE is the energy separation between these states and g is the degeneracy factor. Hence, since the strength of the CISL transition is proportional to $(N_1 + N_2)$ while that of the VISL transition is proportional to N_2, we find

$$\frac{\mathcal{A}_{VISL}}{\mathcal{A}_{CISL}} \propto \frac{N_2}{N_1 + N_2} = \frac{1}{1 + (1/g)e^{\Delta E/kT}}, \tag{1}$$

where $\mathcal{A}$ indicates the PIA. In Fig. 4 we show the ratio between the VISL and CISL integrated PIA versus temperature for various QD sizes. Despite the limited range of our experimental data (which are limited by the relatively weak VISL absorption at temperatures lower than 100–150 K), we can fit the experimental data to Eq. (1) and deduce the activation energies ΔE. The results are shown in the inset of Fig. 4. Notice that the measured energy differences between the lowest two valence sublevels are in the range of 40–80 meV, below the spectral range of our experimental setup. The energy difference between the lowest valence sublevels increases with decreasing size of the QDs as can be expected from a quantum confinement model.

Let us discuss now possible explanations for the origin of the above valence sublevels. First, assuming a spherical symmetry of the valence sublevels as predicted by the $\vec{k} \cdot \vec{p}$ model, we suggest that the ground valence sublevel is essentially composed of the $1S_{3/2}^h$ state while the $1P_{3/2}^h$ and the $2S_{3/2}^h$ states are related to the first and second hole excited sublevels, respectively.[17] Higher order excited states either are above the energy range of our measurements or have significantly lower ISL oscillator strengths. Following the ISL symmetry based selection rules then, only the $1S_{3/2}^h \rightarrow 1P_{3/2}^h$ and the $1P_{3/2}^h \rightarrow 2S_{3/2}^h$ transitions are allowed. However, in our experiment only the second VISL transition has been observed at moderate temperatures where the $1P_{3/2}^h$ sublevel is thermally populated. We would like to emphasize that it is the assumption of spherical symmetry of the QD envelope states that prohibits the $|1h\rangle \rightarrow |3h\rangle$ VISL transition in agreement with our findings. Another possible explanation for our experimental data can be derived by assuming the presence of a surface localized hole state that efficiently traps carriers at energies slightly below the QD band gap.[23] In this case, the measured activation energy is related to the trap confinement energy as measured relative to the valence ground state. Notice that this energy is also expected to increase with decreasing size of the nanocrystals. Such a trap

could be formed, for example, at the InAs QD surface due to incomplete ligand passivation.[23,24]

In conclusion, we have observed two groups of ISL transitions in colloidal InAs QDs. The first group of CISL transitions persists at all temperatures while the second group of VISL transitions is thermally activated and appears at temperatures above 100 K. The identification of these transitions is based on the excellent agreement between the measured ISL transition energies and those obtained from STM and PLE spectra. The origin of these transitions can be explained either by assuming well-defined symmetry based ISL selection rules for our InAs QDs with radii down to 1.4 nm, or by assigning the thermal activation of VISL transitions to the presence of a surface localized state at the IaAs QD surface.

---

*Corresponding author. Electronic address: saar@vms.huji.ac.il

[1] A. P. Alivisatos, Science **271**, 933 (1996).

[2] M. A. Kastner, Phys. Today **46**, 24 (1993).

[3] M. G. Bawendi, W. L. Wilson, L. Rothberg, P. J. Carroll, T. M. Jedju, M. L. Steigerwald, and L. E. Brus, Phys. Rev. Lett. **65**, 1623 (1990); C. B. Murray, D. B. Norris, and M. G. Bawendi, J. Am. Chem. Soc. **115**, 8706 (1993).

[4] P. Moriarty, Rep. Prog. Phys. **64**, 297 (2001).

[5] M. G. Bawendi, P. J. Carroll, W. L. Wilson, and L. E. Brus, J. Chem. Phys. **96**, 946 (1992); C. B. Murray, D. B. Norris, and M. G. Bawendi, J. Am. Chem. Soc. **115**, 8706 (1993).

[6] D. J. Norris and M. G. Bawendi, Phys. Rev. B **53**, 16 338 (1996).

[7] U. Banin, C. J. Lee, A. A. Guzelian, A. V. Kadavanich, A. P. Alivisatos, W. Jaskolski, G. W. Bryant, Al. L. Efros, and M. Rosen, J. Chem. Phys. **109**, 2306 (1998).

[8] E. Lifshitz, I. D. Litvin, H. Porteanu, and A. A. Lipovskii, Chem. Phys. Lett. **295**, 249 (1998).

[9] M. Leon, P. M. Petroff, D. Leonard, and S. Fafard, Science **267**, 1966 (1995); S. A. Empedocles, D. J. Norris, and M. G. Bawendi, Phys. Rev. Lett. **77**, 3873 (1996).

[10] E. E. Vdovin *et al.*, Science **290**, 122 (2000).

[11] U. Banin, Y. W. Cao, D. Katz, and O. Millo, Nature (London) **400**, 542 (1999); O. Millo, D. Katz, Y. W. Cao, and U. Banin, Phys. Rev. B **61**, 16 773 (2000).

[12] H. Drexler, D. Leonard, W. Hansen, J. P. Kotthaus, and P. M. Petroff, Phys. Rev. Lett. **73**, 2252 (1994).

[13] S. Sauvage, P. Boucaud, F. H. Julien, J. M. Gérard, and V. Thierry-Mieg, Appl. Phys. Lett. **71**, 2785 (1997).

[14] P. Guyot-Sionnest and M. A. Hines, Appl. Phys. Lett. **72**, 686 (1998).

[15] H. Fu, L.-W. Wang, and A. Zunger, Phys. Rev. B **57**, 9971 (1998); A. J. Williamson and A. Zunger, *ibid.* **61**, 1978 (2000).

[16] S. Lee, J. Kim, L. Jonsson, J. Wilkins, G. W. Bryant, and G. Klimeck, Phys. Rev. B **66**, 235307 (2002).

[17] Al. L. Efros and M. Rosen, Annu. Rev. Mater. Sci. **30**, 475 (2000).

[18] T. Richard, P. Lefebvre, H. Mathieu, and J. Allegre, Phys. Rev. B **53**, 7287 (1996).

[19] A. A. Guzelian, U. Banin, A. V. Kadavanich, X. Peng, and A. P. Alivisatos, Appl. Phys. Lett. **69**, 1432 (1996).

[20] M. Olszakier, E. Ehrenfreund, E. Cohen, J. Bajaj, and G. J. Sullivan, Phys. Rev. Lett. **62**, 2997 (1989).

[21] S. Calderon, O. Kadar, A. Sa'ar, A. Rudra, E. Martinet, K. Leifer, and E. Kapon, Phys. Rev. B **62**, 9935 (2000).

[22] J. B. Xia, Phys. Rev. B **40**, 8500 (1989).

[23] C. McGinley, M. Riedler, T. Moller, H. Borchert, S. Haubold, M. Haase, and H. Weller, Phys. Rev. B **65**, 245308 (2002).

[24] O. I. Micic and A. G. Nozik, J. Lumin. **70**, 95 (1996).